# Liquid hydrogen structure factor to 5 GPa and evidence of a crossover between two density evolutions

Gunnar Weck,[1] Gaston Garbarino,[2] Paul Loubeyre,[1] Frédéric Datchi,[3] Thomas Plisson,[1] and Mohamed Mezouar[2]

[1]*CEA, DAM, DIF, F-91297 Arpajon, France*

[2]*European Synchrotron Radiation Facility, Boîte Postale 220, 38043 Grenoble, France*

[3]*Institut de Minéralogie, de Physique des Matériaux et de Cosmochimie (IMPMC), Sorbonne Universités - UPMC Univ. Paris 6,*
*CNRS UMR 7590, IRD UMR 206, MNHN, 4 place Jussieu, F-75005 Paris, France*

The center-of-mass structure factor, $S(Q)$, of liquid hydrogen and liquid deuterium has been measured up to 5 GPa, mostly along the melting line from 50 to 296 K. Good quality data were achieved thanks to a novel synchrotron x-ray technique that can isolate the very weak x-ray scattering signal of the micrometric volume of hydrogen compressed in the diamond anvil cell. $S(Q)$ is dominated by a broad peak and hence, its wave-vector position, $Q_m$, is used to appreciate the structural changes in the system. An isotope effect in the position of $Q_m$ is observed that can be explained by a density effect. The shift of $Q_m$ towards higher $Q$ as density increases is followed over a threefold compression. Two simple liquid type evolutions are disclosed with a crossover between them around 37 nm$^{-3}$/molecule. An interpretation is proposed based on the change in the zero-point motional renormalization of the interaction from anharmonic to harmonic.

Understanding the structural and dynamical properties of liquid hydrogen is of fundamental interest, not only at low temperature where the hydrogen isotopes represent the most relevant examples of a Boltzman quantum liquid [1] but also at high pressure where subtle structural changes in the liquid could explain the maximum on the melting curve [2] or be directly related to the mechanism of the transition to the conductive state [3]. This research is also of applied interest, considering the growing importance of liquid hydrogen as an energy carrier or as a fuel for inertial confinement fusion.

Up to now, structural measurements in fluid hydrogen have only been achieved near ambient pressure at low temperatures. The structure factor has been obtained by neutron diffraction [1,4,5] and inelastic x-ray scattering [6]. The extension of these measurements to high pressure presents a formidable challenge due to a strong reduction of the sample volume (required for sample confinement stability) and to the existence of a high background signal coming from the pressure chamber, that combine to drastically reduce the signal to background ratio. Here, we present the measurements of the structure factor of liquid $H_2$ and $D_2$ up to 5 GPa in the diamond anvil cell (DAC). The quality of the data on these micrometric samples is comparable to the one achieved by neutron diffraction on millimetric samples. A discontinuity in the evolution with density of the main diffraction peak wave vector ($Q_m$) shows a crossover between two simple liquid type regimes and its relation to nuclear quantum effects is questioned.

Nuclear quantum effects (NQE) in liquid $H_2$ are expected to endure over a considerable range of temperature and pressure. The importance of NQE can be qualitatively gauged by the ratio of the proton thermal de Broglie wavelength or its molecular counterpart, which expresses the delocalization of the center of mass of $H_2$, over the nearest-neighbor distance between molecules. Going from the low temperature liquid $H_2$, at 15 K and 1 bar, to the liquid near the suspected maximum on the melting curve, about 1000 K and 100 GPa, this ratio

is only reduced by a factor 4. NQE are certainly important at low temperature where they appear in the shift of $Q_m$ to smaller value, indicative of a less close-packed liquid structure than its classical analog at the same density, in the large self-diffusion coefficient and in the anomalous temperature dependence of thermal conductivity and shear viscosity [7,8]. Computational methods to predict these anomalous properties are still under development [9]. Also, at very high pressure, NQE have been shown to significantly shift the predicted pressure of the plasma phase transition [10] and that of the maximum on the melting curve [11]. The isotope effect and the pseudotransition here observed are, respectively, obvious and more subtle manifestations of NQE in liquid hydrogen under pressure.

The difficulty in measuring the structural properties of liquid hydrogen by x-ray diffraction stems from two effects: the small coherent cross section of the hydrogen atom and the presence of a molecular form factor that attenuates the coherent signal at large angles and gives rise to a comparatively larger contribution of the incoherent scattering. The intrinsic small scattering coherent signal is even more problematic at high pressure in the diamond anvil cell because of the small sample volume and of the overwhelming Compton scattering coming from the diamond anvils. Recently, we have developed a method to significantly reduce this background contribution [12]. It is based on the utilization of a multichannel collimator (MCC) device, positioned ahead of a bidimensional x-ray detector, which can isolate a small scattering volume around the sample. The high selectivity of this device has proven essential to extract the structure factor of liquid hydrogen and deuterium over an extended pressure-temperature domain, as reported below. Experiments were carried out at the ID27 beamline of the European Synchrotron Radiation Facility. It should be noted that the analysis of the diffracted signal to extract $S(Q)$ is independent of the isotope, in contrast to neutron diffraction, and consequently relative effects between $H_2$ and $D_2$, i.e., isotopic differences in $S(Q)$ due to NQE, should be meaningful.

Two samples of liquid $H_2$ and one sample of liquid $D_2$ were loaded in a membrane DAC, equipped with Boehler-Almax designed diamond anvils with a large x-ray aperture ($2\theta_{max} = \pm 35°$). The liquid was confined in a CuBe gasket and the sample thickness was about 50 $\mu$m at 5 GPa. The diffraction experiment was performed in the transmission geometry with a doubly focused monochromatic x-ray beam of 6 $\mu$m diameter. The diffraction patterns were collected on a MAR345 image plate and integrated with the FIT2D software [13]. The x-ray wavelength was 0.6170 Å (20 keV), selected by taking into account that the coherent scattering cross section of hydrogen rapidly decreases with energy but also that the anvils absorption increases sharply below 20 keV. This is illustrated in Fig. 1(a) which compares the raw spectra obtained with the empty DAC (black) and the loaded one (red) at two different x-ray wavelengths, for an exposure time of 180 s. For a wavelength of 0.3738 Å (33 keV), the liquid signal is only a small fraction of the background even with the MCC device, whereas at 0.6170 Å (20 keV) the main diffraction peak of liquid hydrogen clearly emerges from the background signal. The thermodynamic $P$-$T$ points where the diffraction signal has been collected, are shown in Fig. 1(b) along with the melting curves of the two isotopes, as reported from previous studies [14,15]. Low temperatures were achieved in a continuous helium flow cryostat. The sample pressure was determined using the ruby pressure scale, with the calibration given in [16], corrected for measurements at low temperature [17].

As seen in Fig. 1(a), even for the optimized conditions of the experiment, i.e., using the MCC device and $\lambda = 0.6170$ Å (20 keV) x-ray beam, the major contribution to the x-ray diffracted signal remains the Compton scattering of the diamond anvils which thus needs to be carefully removed. The incoherent scattering from the sample and the contribution of the MCC should also be properly taken into account. This is performed using a self-contained analysis procedure specially developed to extract the structure factor of a liquid in a DAC [18]. This analysis has been validated on liquid argon and water near ambient pressure and subsequently applied to liquid $O_2$ and $H_2O$ over an extended $P$-$T$ range [19,20]. Moreover, this analysis has been recently extended to account for the transmission of the MCC device [12]. The coherent scattering signal can be written as the product of the squared molecular form factor and the center-of-mass structure factor in a free rotor model description. The spherically averaged molecular form factor was calculated with a frozen molecule formulation (with an intramolecular distance fixed at $d_{\text{H-H}} = 0.74$ Å) and a modified atomic scattering factor was used to reproduce the change of the electron density upon formation of the hydrogen molecule from the isolated hydrogen atoms [21].

Typical center-of-mass static structure factors measured in liquid $H_2$ and in liquid $D_2$ are presented in Fig. 2. Although the measured diffraction patterns extend up to 80 nm$^{-1}$, the $S(Q)$ are extracted only up to a $Q_{max}$ value of 50 nm$^{-1}$, since the liquid signal is too weak compared to the background signal above this value. $S(Q)$ is dominated by the main diffraction peak (MDP), in between 23 nm$^{-1}$ and 29 nm$^{-1}$ and in some cases has an undulation around 40 nm$^{-1}$. The MDP height increases near the melting line reflecting the increase of long-range correlations, as expected. The MDP has
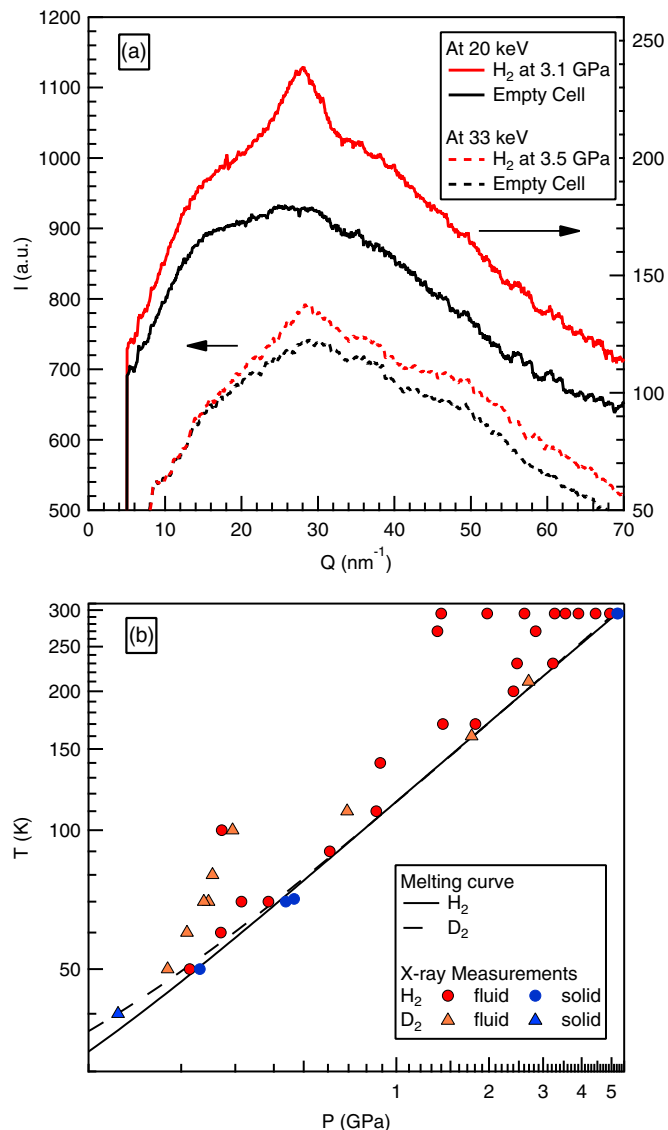


FIG. 1. (Color online) (a) X-ray diffraction spectra of liquid hydrogen in the DAC recorded with the MCC device at two x-ray energies for an exposure time of 180 s. Dashed lines are spectra collected at 33 keV (left scale). Full lines are spectra collected at 20 keV (right scale). Red lines are raw liquid $H_2$ data. Black lines are the empty cell measurements. (b) $T$-$P$ domain covered by the measurements. Full circles and triangles represent the thermodynamic conditions where spectra have been collected on hydrogen and on deuterium, respectively. Red and blue color indicates the liquid and the solid phases. Full line (dashed line) is a Simon equation adjusted on the melting curve of hydrogen (deuterium) measured by Diatschenko *et al.* [15].

a maximum value of 2.2 ± 0.1 for the more structured $S(Q)$. As seen in Fig. 2, the $S(Q)$ measured here at the lowest density is in good agreement with previous neutron determinations obtained near the critical point, which show a maximum value of 2.17 and 2.4 for hydrogen and deuterium, respectively [1,4]. The larger intensity of the MDP of liquid deuterium was interpreted as a signature of a more extended structure and attributed to the smaller zero-point motion of the deuterium molecule with respect to that of hydrogen [22]. In contrast
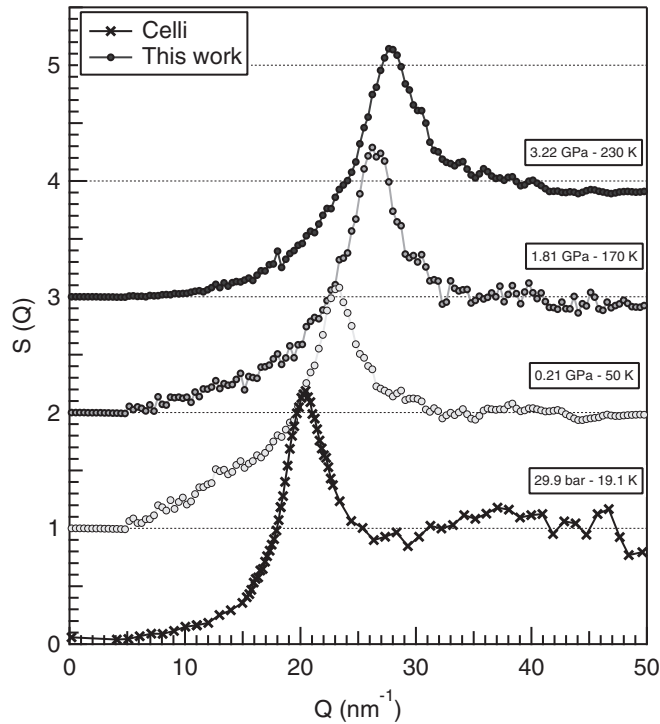
FIG. 2. Intermolecular structure factors of liquid hydrogen ($H_2$) obtained at various temperatures along the melting curve. The curves are vertically shifted by 1. The neutron data of Ref. [1] are shown at the bottom.
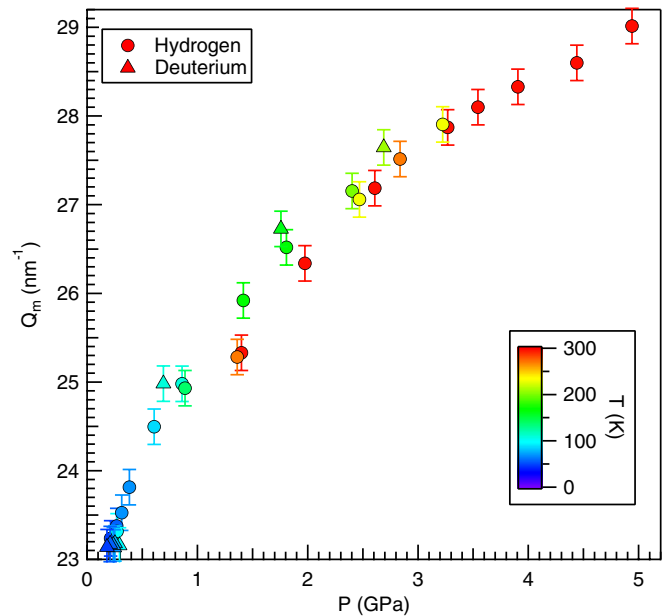


FIG. 3. (Color online) Evolution with pressure of the main diffraction peak position for the hydrogen (full circle) and deuterium (full triangle) structure factors. The temperature is given by the color scale.
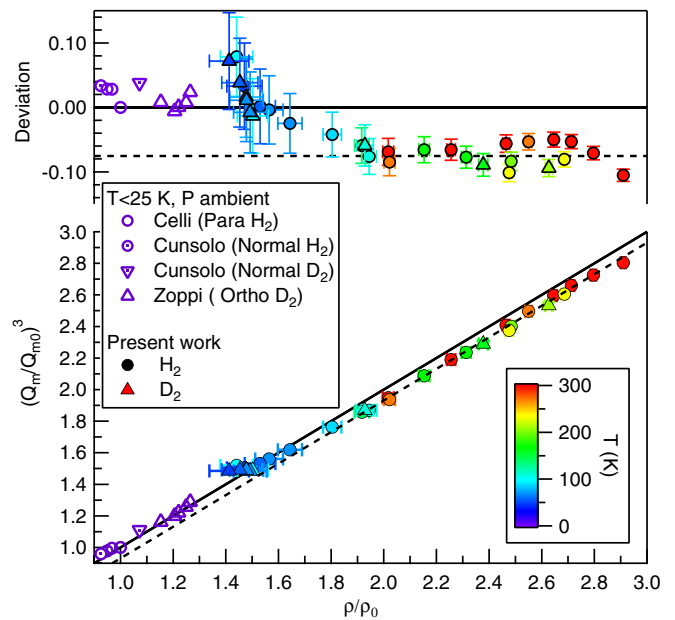


FIG. 4. (Color online) $(Q_m/Q_{m_0})^3$ plotted against $\rho/\rho_0$ where $Q_m$ represents the position of the main peak in the hydrogen (circle) and deuterium (triangle) structure factors and $\rho$ is the liquid density. Full triangles and circles are the present data for $D_2$ and $H_2$. Temperature is given by the color scale. Open circles, open triangles, and dotted symbols are the data from [1], [24], and [25], respectively. The density is obtained from the equation of state [26] for hydrogen at ambient temperature and from the equations of state for hydrogen and deuterium at low temperature [27,28]. The full (dashed) is a guide for the eyes to illustrate the low (high) density linear dependency of $(Q_m/Q_{m_0})^3$ with $\rho/\rho_0$.

here, no difference in the shape of the main peak between the $S(Q)$ of liquid $H_2$ and of liquid $D_2$ is detected within the accuracy of our measurements at similar $P$-$T$ conditions. That indicates a diminution under pressure of the smoothing of $S(Q)$ by NQE.

The wave vector of the MDP, $Q_m$, is plotted versus pressure in Fig. 3 for both isotopes with a temperature color scale. $Q_m$ is strongly shifting with pressure, varying by more than 30% in between 0.5 and 5 GPa. By contrast, $Q_m$ decreases with temperature, and this is more visible at 1.5–2 GPa. An isotopic shift is also observed with slightly larger $Q_m$ for $D_2$ than for $H_2$ under the same $P$-$T$ conditions. A similar isotopic shift was already reported in previous measurements performed at low temperature near the critical point [6,22]. In dense simple liquids, it is empirically found that $Q_m$ is related to the density $\varrho$ through the relation $Q_m \approx 4.4(4\pi\rho/3)^{1/3}$ [23]. Therefore, it is interesting to investigate if the evolution of $Q_m$ in Fig. 3 can be rationalized by the sole density change.

In Fig. 4, $Q_m$ is plotted versus density in a normalized way as $(Q_m/Q_{m_0})^3$ versus $\rho/\rho_0$. The density is estimated from previous accurate measurements of the equation of state of liquid $H_2$ and $D_2$ up to 2 GPa [27,28] and extended to 5 GPa for liquid $H_2$ [26]. The reference values, and $\rho_0 = 22.95$ nm$^{-3}$, are taken from Ref. [1] and correspond to liquid parahydrogen at $P = 29.9$ bars and $T = 17.1$ K. The present set of data points is completed by those obtained previously below 0.05 GPa and below 30 K by neutron diffraction [1,4] and x-ray inelastic scattering [25]. An interesting result in Fig. 4 is that all the data points fall on the same curve. The shifts of $Q_m$ with pressure, with temperature, and with the isotope can thus be explained

by the dependence on density. However, the data points do not fall on a straight line as is the case for a simple liquid. In fact, two linear behaviors are disclosed with a crossover around $37$ nm$^{-3}$. The crossover rather than a sharp discontinuity between the low and the high density structural behaviors could be heuristically interpreted as a pseudotransition between two liquids.

The prevailing picture to understand the interactions in dense hydrogen is that in the $J = 0$ rotational state the molecular distribution of nuclei is spherical, while in the $J = 1$ rotational state it is anisotropic. Consequently, the anisotropic interaction between $H_2$ or $D_2$ molecules depends on the $J = 1$ concentration. The neutron low density data points, plotted in Fig. 4, have been obtained both on the pure $J = 0$ state (para-$H_2$ or ortho-$D_2$) and also in liquids with the $J = 1/J = 0$ concentration corresponding to equilibrium room temperature (normal) value (i.e., 3/4 and 1/3 for $H_2$ and $D_2$, respectively). No difference is observed, reflecting the fact that, in the corresponding density range, the anisotropic interaction is too weak to structure an orientational order of the liquid. The present data have been obtained on liquids with the normal concentration since below 5 GPa the conversion rate between $J = 0$ and $J = 1$ states should be very slow [29,30]. It has been shown that the anisotropic interaction is dominated by the electric quadrupole-quadrupole interaction up to at least 40 GPa and so it should change rapidly under compression, as $\varrho^{5/3}$ [31]. Therefore, at the density of the transition, the strength of the anisotropic interaction has increased by a factor 10 and that could be sufficient to induce a structural modification of the liquid. The shift of $Q_m$ to lower values would hence reveal a reduction of the compacity of the liquid due to orientational correlations between nearest-neighbor molecules. However, that interpretation is not entirely satisfactory because there is no difference between $H_2$ and $D_2$ in Fig. 4 although they have different $J = 1/J = 0$

normal concentration ratio. Furthermore, the orientational ordering in the liquid would occur at a much lower pressure than in the solid [32]. The other interpretation is based on the fact that the nearest-neighbor molecular distance at $34$ nm$^{-3}$ is $\sim 3.4$ Å, which is the value corresponding to the minimum of the semiempirical isotropic potential between molecules [33]. In solid and liquid hydrogen near ambient pressure, the large zero-point motion and anharmonicity of the potential lead to a localization of the molecules at larger distances than the minimum of the intermolecular potential. Under pressure, when the nearest-neighbor distance becomes located in the repulsive part of the potential, the zero-point displacement of the molecules decreases in amplitude and becomes harmonic [33]. Hence the observed crossover in the evolution of $Q_m$ versus density around $37$ nm$^{-3}$ could reflect the change of zero-point motional renormalization of the interaction going from anharmonic to harmonic.

Summarizing, this study presents an accurate determination of the structure factor of liquid $H_2$ and $D_2$ up to 5 GPa in a DAC. A pseudotransition between two liquids, possibly due to the NQE, is disclosed. We hope that this will stimulate quantum simulations to unveil the quantitative microscopic interpretation. Finally, the extension of the present experimental investigation in liquid hydrogen up to the 100 GPa range seems now very encouraging since the sample thickness, hence the signal/background ratio, will only be reduced by a factor 5. This opens up the exciting perspective of investigating liquid $H_2$ near the melting curve maximum where structural changes are expected [2].

---

[1] M. Celli, U. Bafile, G. Cuello, F. Formisano, E. Guarini, R. Magli, M. Neumann, and M. Zoppi, Phys. Rev. B **71**, 014205 (2005).

[2] S. A. Bonev, E. Schwegler, T. Ogitsu, and G. Galli, Nature (London) **431**, 669 (2004).

[3] M. A. Morales, C. Pierleoni, E. Schwegler, and D. M. Ceperley, Proc. Natl. Acad. Sci. USA **107**, 12799 (2010).

[4] M. Zoppi, U. Bafile, E. Guarini, and F. Barocchi, Phys. Rev. Lett. **75**, 1779 (1995).

[5] J. Dawidowski, F. J. Bermejo, M. L. Ristig, B. Fåk, C. Cabrillo, R. Fernández-Perea, K. Kinugawa, and J. Campo, Phys. Rev. B **69**, 014207 (2004).

[6] A. Cunsolo, D. Colognesi, M. Sampoli, R. Senesi, and R. Verbeni, J. Chem. Phys. **123**, 114509 (2005).

[7] F. Bermejo, K. Kinugawa, C. Cabrillo, S. Bennington, B. Fåk, M. Fernåndez-Diaz, P. Verkerk, J. Dawidowski, and R. Fernåndez-Perea, Phys. Rev. Lett. **84**, 5359 (2000).

[8] Y. Yonetani and K. Kinugawa, J. Chem. Phys. **120**, 10624 (2004).

[9] K. Hyeon-Deuk and K. Ando, J. Chem. Phys. **140**, 171101 (2014).

[10] M. A. Morales, J. M. McMahon, C. Pierleoni, and D. M. Ceperley, Phys. Rev. Lett. **110**, 065702 (2013).

[11] L. Caillabet, S. Mazevet, and P. Loubeyre, Phys. Rev. B **83**, 094101 (2011).

[12] G. Weck, G. Garbarino, S. Ninet, D. Spaulding, F. Datchi, P. Loubeyre, and M. Mezouar, Rev. Sci. Instrum. **84**, 063901 (2013).

[13] A. P. Hammersley, S. O. Svensson, M. Hanfland, A. N. Fitch, and D. Hausermann, High Pressure Res. **14**, 235 (1996).

[14] F. Datchi, P. Loubeyre, and R. LeToullec, Phys. Rev. B **61**, 6535 (2000).

[15] V. Diatschenko, C. W. Chu, D. H. Liebenberg, D. A. Young, M. Ross, and R. L. Mills, Phys. Rev. B **32**, 381 (1985).

[16] F. Datchi, R. LeToullec, and P. Loubeyre, J. Appl. Phys. **81**, 3333 (1997).

[17] D. D. Ragan, R. Gustavsen, and D. Schiferl, J. Appl. Phys. **72**, 5539 (1992).

[18] J. Eggert, G. Weck, P. Loubeyre, and M. Mezouar, Phys. Rev. B **65**, 174105 (2002).

[19] G. Weck, P. Loubeyre, J. Eggert, M. Mezouar, and M. Hanfland, Phys. Rev. B **76**, 054121 (2007).

[20] G. Weck, J. Eggert, P. Loubeyre, N. Desbiens, E. Bourasseau, J.-B. Maillet, M. Mezouar, and M. Hanfland, Phys. Rev. B **80**, 180202 (2009).

[21] R. F. Stewart, E. R. Davidson, and W. T. Simpson, J. Chem. Phys. **42**, 3175 (1965).

[22] M. Zoppi, J. Phys.: Condens. Matter **15**, 1047 (2003).

[23] A. Bhatia and N. March, Phys. Chem. Liq. **13**, 313 (1984).

[24] M. Zoppi, A. Soper, R. Magli, F. Barocchi, U. Bafile, and N. Ashcroft, Phys. Rev. E **54**, 2773 (1996).

[25] A. Cunsolo, G. Pratesi, and D. Colognesi, J. Low Temp. Phys. **129**, 117 (2002).

[26] G. Pratesi, L. Ulivi, F. Barocchi, P. Loubeyre, and R. LeToullec, J. Phys.: Condens. Matter **9**, 10059 (1997).

[27] R. L. Mills, D. H. Liebenberg, J. C. Bronson, and L. C. Schmidt, J. Chem. Phys. **66**, 3076 (1977).

[28] R. L. Mills, D. H. Liebenberg, and J. C. Bronson, J. Chem. Phys. **68**, 2663 (1978).

[29] M. G. Pravica and I. F. Silvera, Phys. Rev. Lett. **81**, 4180 (1998).

[30] J. H. Eggert, E. Karmon, R. J. Hemley, H.-K. Mao, and A. F. Goncharov, Proc. Natl. Acad. Sci. USA **96**, 12269 (1999).

[31] P. Loubeyre, M. Jean-Louis, and I. F. Silvera, Phys. Rev. B **43**, 10191 (1991).

[32] G. Geneste, M. Torrent, F. Bottin, and P. Loubeyre, Phys. Rev. Lett. **109**, 155303 (2012).

[33] I. F. Silvera, Rev. Mod. Phys. **52**, 393 (1980).